Initial attitude acquisition in-orbit status of ALSAT-2A remote sensing satellite

HAIDER BENZENIAR
Satellite Engineering Department
Centre de Développement des Satellites
POS 50 Ilot T12, Bir El Djir, Oran
ALGERIA
hbenzeniar@asal.dz

Abstract: - In this paper we present the in orbit performance during the initial attitude acquisition, immediately after separation from the final stage of the launcher, until the satellite converges toward a sun pointing.
On 12th july 2010 ALSAT-2A microsatellite was launched into a 670 km sun synchronous orbit, with a solar local time at an ascending node of 22h15.
In the initial acquisition mode or even in t he safe mode, only sun sensors and m agnetometer are used for attitude determination. Knowing that, t he satellite once is separated from the launcher it starts tumbling. So, as to detumble the satellite, a strategy consisting of three phases is set. The first phase consists on reducing the velocity using only the magnetorquers, until reaching the threshold angular momentum of 0.05 Nms, once this is done, the second phase is automatically enabled in such a way, the four reaction wheels are ON and speed up to get an angular m omentum of -0.15 Nms along the sate llite x-axis. At the end of this phase the satel lite is completely detumbled and a third phase is carried out, in which the satellite minus X axis is pointed toward sun with a small rotation.

Key-Words: - ALSAT-2A, Detumbling, Magnetorquers, Reaction Wheels, Sun pointing,

Received: December 19, 2018. Revised: January 10, 2020. Accepted: March 7, 2020. Published: March 16, 2020.

1 Introduction

Algeria, under the leadership of the Algerian Space Agency ASAL has set up a know how transfer program to develop a space observation sy stem called ALSAT-2. ALSAT-2 system is a constellation of two identical satellites ALSAT-2A and ALSAT-2B. It delivers a high resolution products consisting of a 2.5m resolution for the panchromatic band, and a 10m resolution for the four multispectral bands, with a 17.5km swath for both modes [1]. It has been launched by PSLV-C15 on 12th July 2010 from Sriharikota, Chennaï (India) at 03h52' UT. In this paper we describe the m ain initial attitude performances from the first contact during the LEOP phase until the convergence of the first acquisition mode in such a way that the solar array is completely pointed toward sun with an angular momentum. The control is done first via three magntorquers after that four reaction wheels are activated to enhance the angular m omentum to overcome the external disturbing torques giving the satellite the ability to converge toward an attitude in which the satellite X-axis is opposite to the sun direction.

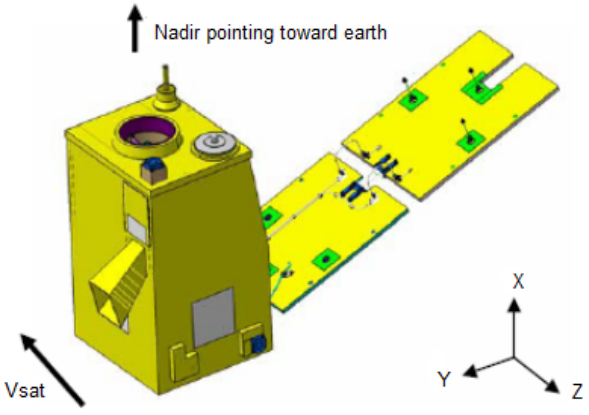

Fig.1 In-flight configuration of ASAT-2A.

2 Satellite Descirption

The structural system of ALSAT-2A has a rectangular configuration for a total satellite mass of 120kg. It consists of payload, and platform . In addition, a deploy able wing solar panel is m ounted on the –Ysat sidewall of the satellite as shown in Fig 1 [2].

The platform part is made up of three plates and four walls and rods. The four walls are made of

honeycomb alloy panels to support the equipments. It is composed of an attitude determination and control subsystem (ADCS), a com munication subsystem composed of an X-band chain dedicated for image data downlink and an S-band chain for telemetry and com mand data. A power subsystem consisting of a GaAs solar array of 180 W, and a 15 Ah Li-ion battery equipped with a management and distribution module, a therm al subsystem, a m ono propellant propulsion subsystem having four thrusters, and a GPS navigation sy stem. All are mounted on the four walls [3].

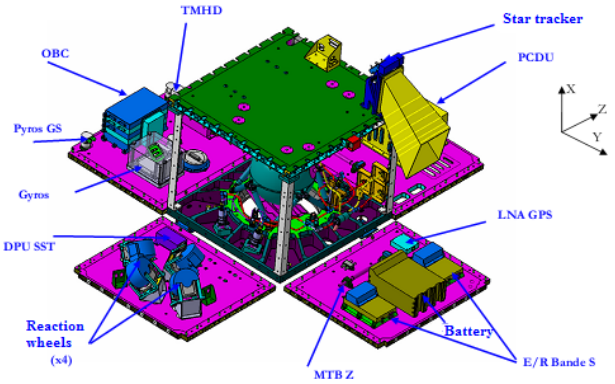

Fig.2 ALSAT-2A in deployable configuration.

3 Acquisition and Safe Hold mode (MAS)

This is the m ode to perform initial attitude acquisition, after launcher separation, and attitude recovery, following failure detected. The Safe Hold mode aims to ensure spacecr aft safety without any ground support [4].
The main design requirements of this mode are:

- To orientate the solar panels and the –Xsat face towards the sun in order to guarantee the generation of electrical power and the payload safehold (thermal control).
- To ensure a slow rotation around the X-axis for thermal reasons.
- To guarantee autonomy from the ground.
- To increase reliability , avoiding use of equipment already used in other modes.

The MAS mode is based on:

- The angular rate esti mation based on magnetometer measurements and on the sun direction when available.
- The estimation of the sun direction and the direction of the eclips e whatever the spacecraft attitude is, using three two axes wide field of view sun sensors.
- A gyroscopic stiffeness around X-axis provided by the four reaction m ounted in a pyramidal configuration, to ensure dyn amic stability despite disturbing torque especially in eclipse.
- MTB (magnetorquer bars) used to control the direction of X-axis with respect to the sun. the magnetic momentum command is defined using the m agnetic field dire ction provided by the magnetometer.

This acquisition and safehold mode is organized in 3 phases as shown in Fig 3.

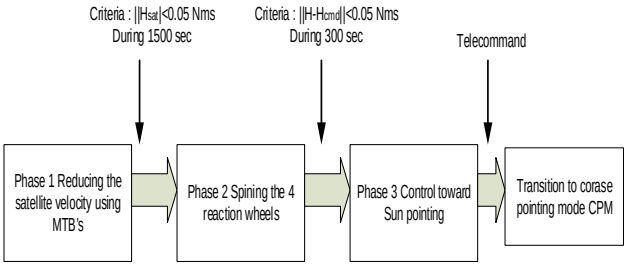

Fig 3. Acquisition and safe mode phases

- ***Phase 1***: in this phase the satellite is tum bling at high rates. So, in order to reduce these rates we call for MTB' s. the angular m omentum is compared to a threshold of m agnitude 0.05 Nm s, and it should fullfil a 1500 sec duration so as to move to the next phase.
- ***Phase 2***: it consists on spinning the 4 wheels at a commanded speed reaching a -0.15 Nms along the x-axis. The difference between the total angular momentum and the com manded angular momentum is compared to a threshold of 0.05 Nms, with a minimum time of 300 sec, to go to the third phase.
- ***Phase 3***: once the satellite is within an acceptable angular momentum, it is then pointed toward sun along its – x-axis.

4 Control law design

As presented previously the Safe Hold m ode is organized in 3 submodes or phases and the control law corresponding to each m ode is described as follows :

4.1 Detumble submode

It is aimed to reduce the initial rates by magnetic damping, in which the two magnetic commands are

controlled to reduce the angular momentum of the satellite. The first magnetic momentum $\overrightarrow{M_1}$ is determined from the derived earth magnetic field $\vec{B}$. The second command $\overrightarrow{M_2}$ is derived from the estimated satellite angular momentum $\overrightarrow{H_{SAT}}$ such that:

$$\vec{M} = \vec{M}_{11} + \vec{M}_{12} = -\frac{I_{SAT}}{\tau_{11} B^2}\dot{\vec{B}} + \frac{\vec{B} \wedge \left(-\frac{\vec{H}_{SAT}}{\tau_{12}} \right)}{B^2} \quad (1)$$

Where:

$\vec{M}$: *Total magnetic momentum.*
$\vec{M}_{11}$: *First term of the magnetic momentum.*
$\vec{M}_{12}$: *Second term of the magnetic momentum.*
I_{SAT} : *Satellite inertia.*
$\vec{B}$: *Earth magnetic field.*
$\dot{\vec{B}}$: *Derived earth magnetic field.*
$\vec{H}_{SAT}$: *Satellite angular momentum.*
τ_{11} : *Filter time constant (first term).*
τ_{12} : *Filter time constant (second term).*

4.2 Reaction wheels spinning submode

This is a transition phase having as an objective to spin up the wheels creating an angular momentum about the X-axis to give to the satellite a sufficient stability in order to be ready for the sun acquisition phase. In this phase, command the MTB with the following:

$$\vec{M}_2 = \frac{\vec{B} \wedge \left(-\frac{\vec{H}_{TOT} - \vec{H}_{cmd}}{\tau} \right)}{B^2} \quad (2)$$

Where:

$\vec{M}_2$: *Total magnetic momentum.*
$\vec{H}_{cmd}$: *Commanded angular momentum.*
$\vec{H}_{TOT}$: *Total angular momentum (satellite + reaction wheel angular momentum).*
τ : *Filter time constant.*

4.3 Sun Acquisition submode

The last phase concerns the sun locking during which the satellite is pointed toward sun. The control is achieved by two commands, the first one controls the total angular momentum to the desired set point, and the second command allows the orientation of the total angular momentum to the sun direction.

$$\vec{M}_3 = \vec{M}_{31} + \vec{M}_{32} \quad (3)$$

Where:

$$\vec{M}_{31} = \frac{\vec{B} \wedge \left(-\frac{\left(\vec{H}_{TOT} - \vec{H}_{cmd} \right)}{\tau_{31}} \right)}{B^2} \quad (4)$$

and

$$\vec{M}_{32} = \frac{\vec{B} \wedge \left(\frac{\left[\vec{H}_{TOT} \wedge \left(\vec{S} \wedge \vec{H}_{TOT} \right) \right]}{\tau_{32} \left\| \vec{H}_{TOT} \right\|} \right)}{B^2} \quad (5)$$

Where:

$\vec{M}_3$: *Total magnetic momentum.*
$\vec{M}_{31}$: *First term of the magnetic momentum.*
$\vec{M}_{32}$: *Second term of the magnetic momentum.*
$\vec{H}_{cmd}$: *Commanded angular momentum.*
$\vec{H}_{TOT}$: *Total angular momentum (satellite + reaction wheel angular momentum).*
$\vec{S}$: *Solar direction unit vector.*
τ_{31} : *Filter time constant (first term).*
τ_{32} : *Filter time constant (second term).*

5 In-Orbit results and discussion

ALSAT-2A has been launched by PSLV-15 on july 12th at 03:52:00 UTC, the injection of the satellite from the launcher occurred 04:11: 09.400 about 1140 seconds. At this moment, the satellite is tumbling at < 3 deg/s on the three axes. At the 1800th second, the solar array was automatically deployed and the initial acquisition mode starts. The main performance requirements of this mode are:

- The convergence duration shall be less than 18000 sec.
- The minus X-Sat axis shall be pointed toward sun better than 30 deg once the satellite is in the convergence phase

In this section, we shall present the in-orbit results obtained from the telemetry, to show the

performances, and how they fulfill the stated requirements. We should notice here that the time used is the OBC (On board com puter) time before we made synchronization.

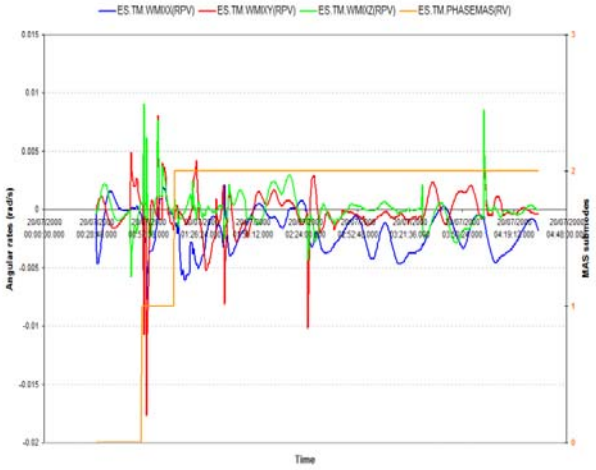

Fig 4. Angular rates vs the initial acquisition sub-modes.

MAS convergence is attained in minimal time, thanks to small angular rate at injection.
According to Fig 4, that il lustrates the evolution of the angular rates issued from the magnetometer and the sun sens ors measurements we notice that the initial rates were about 0.01 deg/sec and the duration of t he first phase was 1502sec lower than the duration obtained du ring simulations. This is mainly due the rate of separation that was about 1deg/sec. Now regarding the peaks observed they occur at the eclipse exit, but the rates converge rapidly.

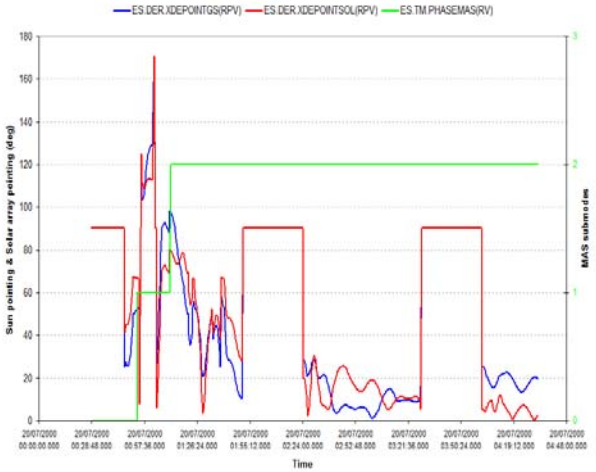

Fig 5. Sun pointing and solar array pointing vs initial acquisition sub modes.

Fig 5, sh ows the evolut ion of the minus X-sat direction toward sun (sun pointin g) and the solar array pointing, just after satellite injection. During the first submodes the high am plitude of the sun pointing error, but at the beginning of the thir d phase the po inting starts to converge and leads to under 30 deg for bot h parameters during the thir d phase.

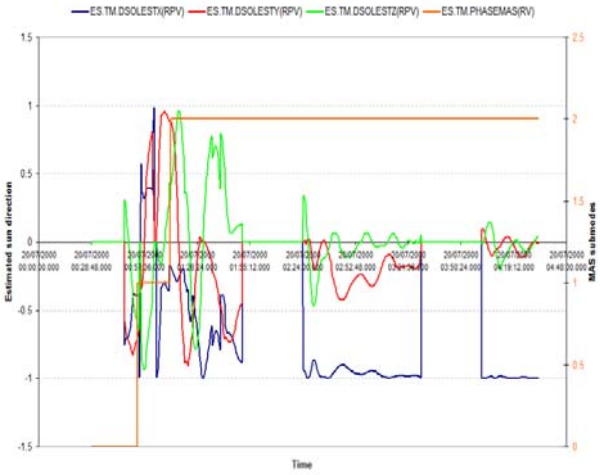

Fig 6. Estimated sun direction vs initial acquisition submodes.

Now, regarding the estimated solar direction a s displayed in Fig 6. We n otice that du ring the first two submodes an important variation of the estimated angle between the minus Xsat axis and the solar direction from the initial acquisition throughout the activation of the reaction wheels until the thir d phase where the convergence leads toward an acceptable.

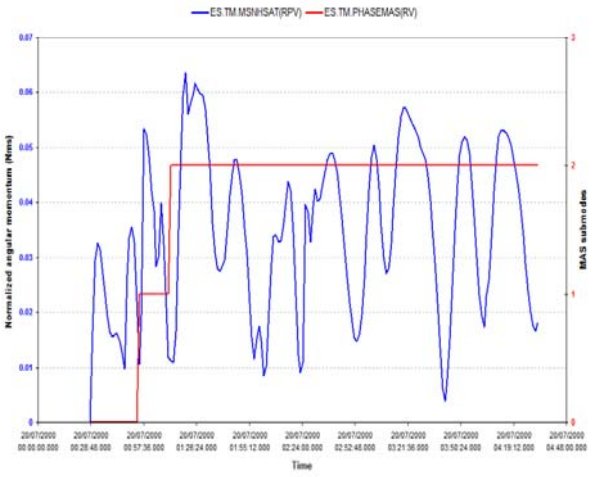

Fig 7. Normalized angular momentum vs initial acquisition sub modes.

The angular momentum and its normalized value are illustrated in Fig 7, and Fig 8, f or the first submode we can notice th at the angular momentum amplitude is under 0.05 Nms and the transition to next phase starts with a peak values this is mainly due to the spin up of the four wheels by creating the angular momentum. The third subm ode is enabled

once and the transition criterion ($\left\|\vec{H}_{sat}-\vec{H}_{cmd}\right\|<0.05Nms$ during 300 sec) is satisfied and we can notice the appearance of peak values caused by changing the control laws from submode to another.

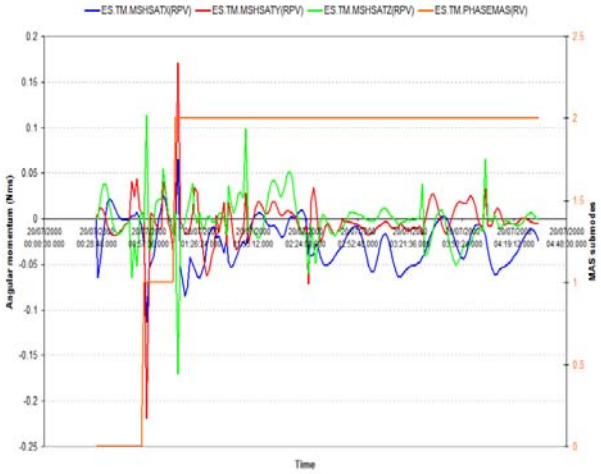

Fig 8. Angular momentum vs initial acquisition sub modes.

OBC time synchronisation has been done in the converged submode corresponding to the july 12th, 2010. The converged MAS mode behaviour is illustrated in Fig 9 displaying the angular rates and the eclipse state, two peaks are observed at beginning of the eclipse phase because of the lack of sun sensors measurement, only magnetometer measurements are available in the eclipse phase.

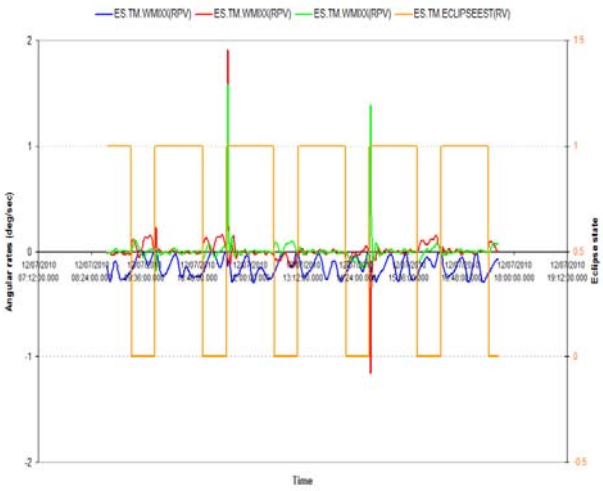

Fig 9. Angular rates vs Eclipse state.

As for the angular rates, and after OBC synchronisation the angular momentum is within its specified values along the three axis (the criterion of $\left\|\vec{H}_{sat}-\vec{H}_{cmd}\right\|<0.05Nms$ is respected). The two peak values observed during this period corresponds to the positions when entering eclipse regions, but these peaks are quickly absorbed due to the high torque generated by the four wheels mounted in pyramidal configuration, and hence generating more torques.

Fig 10. Angular momentum.

Table 1, represents the in-flight duration of each submode compared with those predicted during the design. According to the obtained durations, we can notice that they are lower than the predicted durations, thanks again to the small rate of injection

Table 1. MAS sub modes duration

	Predicted duration (sec)		In flight duration (sec)
	Min	Max	
MAS phase 1	1500	20000	1502
MAS phase 2	600	1500	1094
MAS phase 3 (*convergence better than 30 deg*)	2200	38900	4700

Fig 11, shows the sun pointing error with respect to the direction of the sun during MAS convergence. Intervals with 90 deg pointing error corresponds to the satellite passing through earth shade.

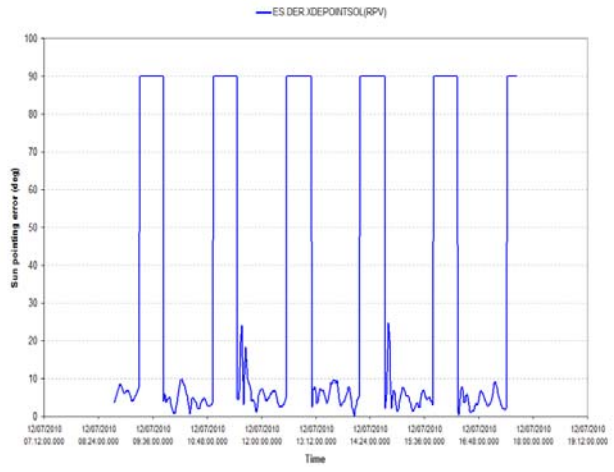

Fig 11. Sun pointing error during the converged initial acquisition sub modes.

Even after convergence is attained, p ointing error greater than 10 deg is periodicall y observed during short periods. This error is caused by solar reflection when entering da y light, which perturbs the estimation of direction.

As it is depicted in Fig 12, the behaviour of the wheels throughout all the initial attitude acquisition submodes from the wh eel activation until the constant speed leading to the convergence state under 30 deg pointing error.

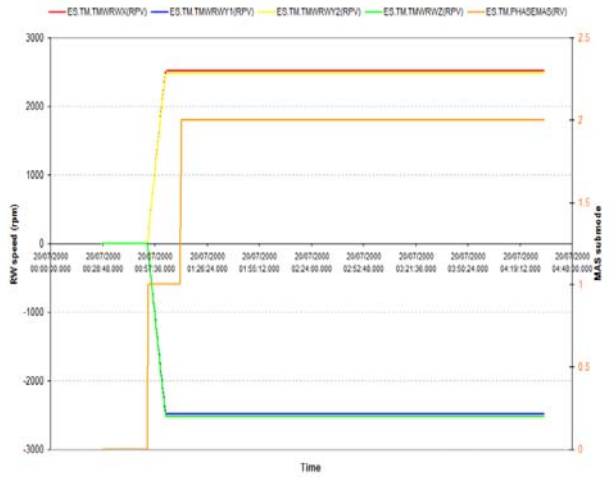

Fig 12. Reaction wheels speed vs initial acquisition sub modes.

4 Conclusion

The purpose of this paper was to represent the flight results during the initial acquisition mode from launcher separation until satellite sun pointing, where the main performances were depicted and discussed.

The convergence of this mode was successfully reached in a minimum time lower than the predicted duration during the design, and satellite was able to go to the next mode.

References:

[1] M. Kameche, A.H. Gicquel, D. Joalland, "ALSAT-2A Transfer and First Year Operations", Journal of Aerospace Engineering, Sciences and Applications, Vol. 3, No. 2, pp. 67-75, May 2011.

[2] G. Limouzin, M. Si guier, A. Chikouche, "AlSat-2 Program - Overview, 1 y ear from launch," International Workshop on Earth Observation Small Satellites for Rem ote Sensing Applications, Kuala Lum pur, Malaysia, Nov.23-27, 2007

[3] N. Larbi, M. Attaba, F. Bouchiba, E. Beaufume, "ALSAT-2A solar array in orbit performances after 32 months", International Symposium on Remote Sensing, Conference on Sensors, Systems, and Next Generation Satellite", Dresden, Germ any ,23-26september 2013.

[4] M. Le Du, J. Maureau, P. Prieur, "Myriade: an adaptative AOCS concep t". 5th inter national ESA conference on Spacecr aft Guidance Navigation and Control S ystems, Frascati, 22-25 October 2002.